



PREDICTION OF THE TUMOR RESPONSE LYMPH NODE BASED ON DEEP RESIDUAL BOLTZMANN CONVOLUTION NEURAL NETWORK

Manu M R¹, T Poongodi*²

Abstract

The most prevalent metastatic location for rectal carcinoma (RC) are lymph nodes (LNs), and the nodal status is crucial to treating and forecasting choices. The site and several metastatic LNs should be investigated before treatment guidelines comply with the NEC Network and the American Joint Committee on Cancer (AJCC) stage standards. Identifying and removing metastatic LNs during the intervention is crucial to prevent tumour repetition, especially in lateral lines. Some studies have shown that stronger LLNs can be closer to local recurrence and showed that dissection of LLNs might enhance prognosis and reduce local recurrence for patients with poor RC at these locations. In contrast, LLND is an autonomous procedure with generally more surgical implications, including surgery and long-term sexual and urinary problems. Therefore, the correct number and position of metastatic LNs must be indicated before surgery in the therapy option. This work deals with segmentation and classification challenges for normal and abnormal lymph nodes. Here Preprocessing is performed by Curvature based shearlet filter with Contrast Limited Savitzky-Golay Histogram Equalization is used. The Semi-Supervised Fuzzy Logic clustering Algorithm was then used to segment lymph nodes. Once the lymph region is segmented, the grey level co-occurrence matrix is used to extract functions (GLCM). Then the scale-down bee herd optimization approach is introduced to minimize the number of measures by features, which increases the classifier detection rate. Deep residual Boltzmann Convolution Neural Network system of classification creates a pattern for the benign lymph nodes and the malignant identification. In comparison to state-of-the-art procedures, the simulation results demonstrate the importance of the proposed method by obtaining a high range of precision (97.7%), sensitivity (95.7%) and specificity (95.8%) than any other existing methodology.

6788

KeyWords: Rectal cancer, Lymph nodes, Curvature based shearlet filter, Contrast Limited Savitzky-Golay Histogram Equalization, Semi-Supervised Fuzzy logic clustering algorithm, Gray Level Co-occurrence Matrix, Scale down Bee herd colony optimization, Deep residual Boltzmann Convolution Neural Network.

DOI Number: 10.14704/nq.2022.20.8.NQ44703

NeuroQuantology 2022; 20(8): 6788-6800

¹ Research scholar, SCSE Galgotias University, Greater Noida, Uttar Pradesh, India, manuramachandran18@gmail.com

² Professor, SCSE Galgotias University, Greater Noida, Uttar Pradesh, India, tpoongodi2730@gmail.com



Introduction

In the Western world, rectal cancer is a prevalent and significant cause of mortality. It forms a substantial portion of gastrointestinal tumours and, although it decreases over the previous two decades, the death rate for colorectal cancer is still high. Metastasis of the Lymph node (LN) is essential in metastatic rectal cancer because, due to substantial local repeatability, it typically leads to a dismal prognosis. To determine the best treatments for individuals who have rectal cancer, a preoperative examination of metastatic LNs is very crucial. Magnetic resonance imaging (MRI) has been widely used in rectal cancer metastatic LN detection and is considered superior to CT to improve soft tissue discrimination. In general, however, radiologists require a lot of effort to detect metastatic LNs by their forms, limits and intensities of the signals. In addition, several radiologists often have varied judgments concerning LN metastases, even on the same MRI imaging. Varying prediction approaches have been developed to improve preoperative metastatic LN identification in colorectal cancer include gene- or serum miRNA-based models and image modelling. Radiomics from CT scans are dominating among image-based models. Different radiomics characteristics are Picked first from radiological imaging of a patient and then blended linearly with a radiomics score. The following questions arise:

- (1) Since MRI is better than CT in the diagnosis of metastatic LNs, how are the models performed from MRIs and
- (2) Are alternative approaches for the quick and accurate assessment of metastatic LNs available on the image?

In the last decade, deep learning technology has been created to recognize photos; the auto-identification of deep learning images has contributed to identifying and labelling the regions of interest using automated sketching approaches and 3D reconstruction. It was employed on the skin, lung, breast and prostate in the diagnosis of solid tumours. However, compared with solid tumours, because of their enormous amounts and minor variations, metastatic LNs are more challenging to detect.

Rectal cancer has made considerable progress with introducing novel adjuvant and neoadjuvant medicines and novel operating procedures such as transanal endoscopic microchirurgie in recent years (TEM). These improvements have made exact nodal stages for rectal cancer ever more critical in directing each patient's multiparametric choice of therapy choices. Confident elimination of nodal involvement might allow for local excisions, such as TEMs in early-stage (T1) patients with lower peri- and post-operative morbidity than traditional procedures. In addition, the correct identification of tumour nodes can identify patients who would benefit either from neoAD or post neoadjuvant chemistry and resection when preoperative therapy prevents an exact identification of pretreatment conditions. Preoperative treatment can also identify patients who would benefit from neonatal chemotherapy before surgery. Currently, MRI is used to stage rectal cancer, which has become the reference standard. The comparatively poor accuracy of nodal staging was assessed with several approaches. A deeper residual Boltzmann Convolution Network has been constructed and trained to identify cancerous lymphoid nodes automatically. Our computer tool can exactly support the input image and make it extremely easy to diagnose. The remaining section of this paper is organized as follows: section 2 depicts various existing methods related to the prediction of rectal cancer via image processing techniques. Section 3 is the depiction of the problem statement. Section 4 illustrates the proposed mechanism. Section 5 is the performance analysis for the proposed scheme. Finally, the overall workflow is concluded in section 6.

RELATED WORKS

[1] A deep neural network (DNN) was created to predict the whole behaviour as a methodological proof of principle. The findings were compared with the linear regression base model with the TNM only as a predictor. The DNN with the supporting vector machine has a second model with identical features. [2] Create survival regression models in the proportional risk model by optimizing imagery characteristics with



profound convolutionary neural networks (CNNs). A spatial pyramid pooling method is implemented to make CNN's relevant to tumours of different sizes. [3] The DL method for rectal cancer prediction is based on kurtosis diffusion, and T2 weighted MRI developed and validated. [4] Proposal of a quicker R-CNN monogram to predict LN's metastatic state, including age prediction, Faster R-CNN metastatic LNs and tumour differentiation levels.[5] Designed the SVM model for addressing this issue by including biomarkers associated with Epithelial-Mesenchymal-Transition (EMT) as well as clinicopathological factors. [6] Radiographical data have been generated from the rectal tumour, LN and endorectal ultrasonography (ERUS) peripheral tissue, computed tomography and wave-elastography of shaking (SWE). Three radiometric values were obtained. An independent predecessor was employed for a multivariate logistic regression and clinical data, followed by a monogram. Compared to classical radionics, the multiparametric monogram was predictive.[7] Report on the preoperative ALN prevention report for Deep Learning Radiomics (DLR) for early-stage breast cancer patients using Elastography Shear Wave and Ultrasound images.[8] The study aimed to demonstrate that the computer algorithm is used by supporting radiologists to quantitatively analyze radiologists' morphological MRI features to estimate local rectal cancer lymph gland presence or absence of metastatic disease. This work supports computer-aided nodal reading but requires more details and validation of larger data sets. [9] A prediction was explored in a clinical study for the tumour stage (tumour, node, or metastasis) of colon cancer utilizing the most relevant histopathological criteria and the five years of DFS-free survival (DFS).[10] It provides the model for the Naïve Bayes Classification as a

technique for classification to demonstrate that the model has high accuracy, excellent accuracy, excellent reminder, excellent f1 – the results of a rating of the colon cancer patient data. In this model provided, Naïve Bayes Classifier is a prediction based on a basic probabilistic and a strong assumption of independence based on applying the Bayes theory (or Bayes rule). This approach can thereby increase the accuracy of categorization with lower complexity. [11] tried to identify colon cancer and forecast a KRAS mutation status in histopathological imagery using machine Apple learning algorithms. They took 250 photos of colon cancer and 250 photos of normal colon tissue. Calculations of KRAS mutational-positive tumours were taken to half of the colon cancer photos and KRAS mutation-negative ones to another half. Then, with the help of the Apple Create ML learning module, they constructed image classification models. [12] A deep neural networking model to detect components of colon cancer tissue has been created in both the Tissues Bank Center and the Pathological Archives of the University of Mannheim. This model was used to collect pictures of patients with colon cancer from the Atlas of Cancer (TCGA). The LNM peripheral tumour stoma prognostic value has been examined (PTS). [13] To provide a new model of noninvasive artificial intelligence based on CT data to prevent colon cancer liver metastases. [14] Provide a colon cancer prediction approach for both the critical kernel and features based on gene expression profile (important genes). T-statistics conducted the selection of functions (genes).[15] Presents a system of colon cancer sensing with transfer learning architectures for automated patient diagnosis and prognosis to automatically extract high-level information from colony biopsy photos—carcinoma through computationally successful means.

S.no	Title	Reference	Algorithm	Advantage	Disadvantage
1.	Deep learning and radionics predict full response for local advanced rectal cancer following neoadjuvant chemoradiation.	[1]	Deep Learning convolution network	Less training time	Less detection accuracy



2.	Deep neural imaging networks based on rectal cancer survival data	[2]	Deep convolutional neural networks	High rate of survival prediction	Mathematical errors are high
3	Prediction of rectal reaction to neoadjuvant chemoradiation with a profound knowledge of diffusion kurtosis MRI	[3]	deep learning	Easy to implement	High image fusion errors
4	A profound learning monogram for the prevision of metastatic rectal cancer lymph nodes	[4]	deep learning	Less training and testing error	Large training data needed
5	Biomarkers of epithelial-mesenchymal transition and vector machinery driven models predict metastases of the regional rectal lymph node.	[5]	CNN	Detect lymph nodes easily	Conventional model SVM can be used without any novelty
6	Multiparameter radiomy improves the spread of rectal cancer in lymph nodes in comparison to traditional radio	[6]	Multiparametric radiomics	High detection ratio	Large training data needed
7	Deeply learned X-rays in the early-stage breast may forecast the condition of the axillary lymph node	[7]	Deep learning	Less training time	High error over image analysis problem
8	A computer-aided lymph node status method for rectal cancer predictions	[8]	Computer-aided algorithm	Less training time	Does not work properly while the database was large
9	Prediction of stage and survival of colon cancer with an approach to machine learning	[9]	Random forest machine learning approach	High detection accuracy	Training time was high
10	Models for the prediction of colon cancer with Naïve Bayes	[10]	Naïve Bayes classifier	Less training time	Errors are high
11	. However, The Apple machine effectively detects colon cancer algorithms KRAS mutation status is not predictable	[11]	Apple machine learning algorithms	High detection accuracy	High detection time
12	Colon cancer Histopathological Images Deep, revolutionary network-based lymph node metastasis	[12]	Deep Convolutional Neural Network	Training time was less	Hard to implement
13	Establishment of a novel noninvasive prediction model for colon cancer liver metastases	[13]	noninvasive model	Very fast	Statistical errors are more
14	Gene expression profile cancer prediction using a kernel-based	[14]	kernel-based support vector	Kernel implementation	Difficult to



	vector supportive machine		machine	leads to high cancer prediction	implement
15	Prediction of Colon cancer with histological pictures and the optimal SVM of Bayesian	[15]	deep-learning features and Bayesian optimized SVM	Easy to integrate process	Less detection accuracy
16	Detection of deep-learning colorectal cancer	[16]	deep learning	Easy to train	Testing time high
17	Colorectal cancer detection varied in image classification using residual network (ResNet)	[17]	ResNet	Computationally faster	High cost

Several methods are previously proposed in the literature to detect colon cancer by identifying the metastatic lymph node, but each has some more disadvantages. Hence to overcome all the existing research gaps, a novel methodology was implemented here.

PROBLEM STATEMENT

In the image analysis using image processing applications, numerous theoretical strategies and methods are produced. While several approaches exist, the key challenges remain a significant challenge in classification and segmentation for the researchers. There is also the need to determine an acceptable methodology to achieve a distinct image for the segmentation process. Usually, owing to disturbances and illuminations, the colon radiology image was not visible clearly. While research findings give many methods for solving this issue, these methods prove costly. Therefore it was possible to classify colon.

PROPOSED METHODOLOGY

Here the segmentation and classification of Colon CT images were done using a deep learning technique focused on disease prediction. The suggested methodology was tested using well-

known controlled and unsupervised approaches for segmentation and classification, consistency and runtime metrics. Throughout the following parts, the deep learning methodology was addressed and the methods included in the segmentation and classification of colon cancer.

CNN method has excellent success in the segmentation, classification and identification of digital image objects. However, CNN has certain drawbacks as each area proposal needs a complete coevolutionary network transfer, broad memory consumption with poor detection speeds. Nonetheless, the usage of CNN is warranted in circumstances that require high precision for object identification but do not need real-time processing. To overcome the existing issues Deep residual Boltzmann Convolution Neural Network model is part of the series of exciting developments of the CNN models. Figure 1 presents the flowchart of the suggested methodology. The first stage called a preprocessing step—the second stage in which the segmentation can be done. After the third stage, the feature extraction can be done. Finally, the process can be concluded with the suggested CNN based classification. On the Cancer Imaging Archive, the proposed method is largely validated.



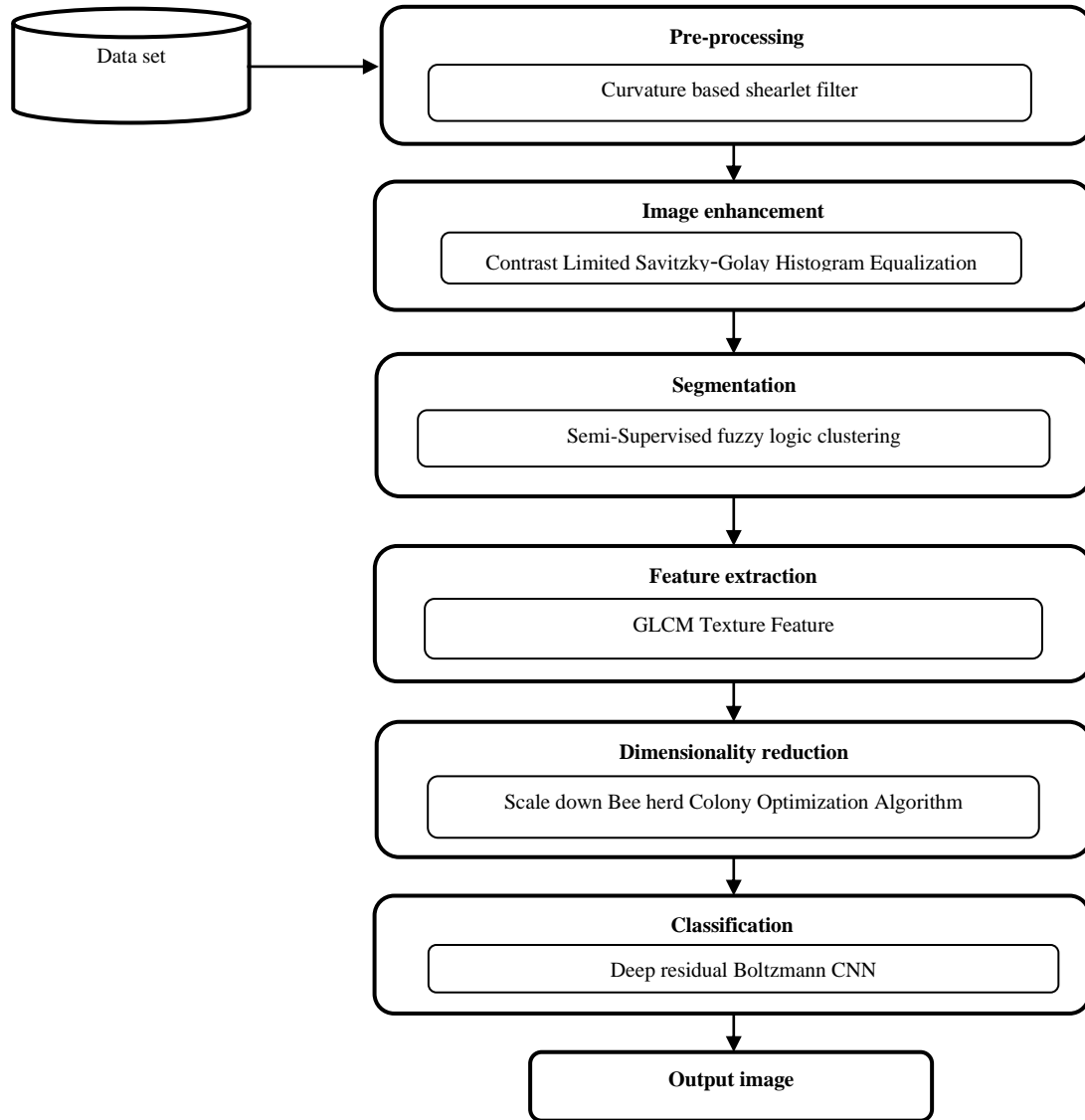


Figure 1 Schematic representation of the suggested methodology

The above figure 1 represents the schematic representation of the suggested methodology.

a.Pre-processing

The image processing should be used as an early stage in an advanced technique. It carries out the error treatment, which helps to estimate pixels in the image but may also shape the Curvature by the impulse noise. With the help of all pixels in a picture, it isolates pixels as noise and its neighbouring pixels. It is most adaptable to the neighbouring pixel size. This technique will replace the median pixel value of the pixels in the neighbourhood passed by a noise labelling test. The Curvature-based shearlet filter is designed to

eliminate impulse noise, smooth out other noises and minimize distortion. The filter's performance is shown in the following steps.

Steps

Level Y: $Y1 = GLCBS - GLmin$

$Y2 = GLCBS - GLmax$

If $Y1 > 0$ and $Y2 < 0$, go to the level B

Else window size should gets increased

If size of the window $< Sizemax$, repeat

level Y

Else output $GLpq$

Level Z: $Z1 = GLpq - GLmin$



Z2 = GLpq - GLmax
 If Z1 > 0 AND Z2 < 0, output GLpq
 Else output GLCBS

Size - Curvature based shearlet filter during operations t helps adjust the size of the area.

Garmin - maximum value of gray level in Sizepq

Lomax - maximum value of gray level in Sizepq

GLmed - median gray levels in Sizepq

GLP - the gray level at coordinates (p, q)

Sizemax - the maximum allowed size of Sizepq

Here which initially in the level X suggested filter can remove the noise, then after noise removal, the Curvature of the image can get shape out fully in level Y. Since the special curvatures are imposed, our filters are 100 or 10000 times faster than traditional solvers in terms of minimizing curvatures. After that histogram of the image can be equalized by using the Contrast Limited Savitzky-Golay Histogram Equalization. Typically, histogram equalization is achieved to increase image consistency. Histogram Equalization is a computerized process used to enhance the contrast of pictures. The most typical sensitivity values are improved effectively, i.e. the image intensity range is broadened. In order to boost relations between regions, it allows less local contrast. Therefore, after the implementation of the suggested histogram equalization, the average contrast of the images is improved.

Let p indicate the normalized histogram of any intensity attainable. That's why it can be represented as,

$$p^y = (\text{Number of the pixel with } y \text{ intensity} / \text{total number of the pixels}) \quad (1)$$

Here, $y=0,1,\dots,y-1$

The histogram equalized image can be defined as

$$H_{i,j} = \text{base}((Y-1) \sum_{y=0}^{b_{i,j}} p^y) \quad (2)$$

where, base represents the nearest integer. This is equivalent to transforming the pixel intensity,

$$\frac{\partial N}{\partial x} \left(\int_0^N pN(x) dz \right) = \partial N(N)(x^{-1})(N) d/dN \quad (3)$$

Here, finally, the probability distributed uniformity function can be represented as $\partial N / \partial x$,

While the result indicates that the equalization process used is exactly flat histograms, it can soften them and improve them.

b.Segmentation

The first stage of feature extraction is segmentation. Image segmentation is the division of an image into several segments. Semi-supervised fuzzy logic clustering Segmentation is aimed at breaking down the colon image into segments. Segmentation of the frames is used to identify points and boundary lines, image curves. Segmentation provides a set of sections representing the whole object or a collection of contours derived from the image. A segmented edge uses the topography analogy. By using this method, the image features can be easily pre-determined. In this research, the intensity of the gradient uses grayscales for the segmentation process. The image velocity gradient has high pixels and low pixels along the boundaries of the object. Finally, the region of interest can be segmented.

$$ROI^{Segmentation} = \sum_{\{i,j\} \in Q_2} V_2(y_i, y_j) \cdot m_i \cdot \log_{b_i} + \gamma \int b_i dx \quad (4)$$

Where $ROI^{Segmentation}$ is the edge-based segmentation, V is the velocity gradient, $[Y_i], y_j$ was the low and high pixel value, m represents the number of pixel blocks in the image, $[\log] (b_i)$ represents the spatial size of the image, γ represents the frequency coefficient of an image, c_i represents the distance of the pixels.

The fundamental job of the proposed methodology is to divide a picture into unoverlapped parts. SEEDS are taken as the input, pixels with comparable features are combined and each seed is produced according to a certain region. Here the similarity index between the two neighborhood pixels can be calculated by using the Euclidean distance as follows,

$$eDIST = \sqrt{eD_r} + \sqrt{eD_g} + \sqrt{eD_b} \quad (5)$$

Where $eD_r = (k(x + i, y + j, 1) + (f(x, y, 1))^2$



$$eD_g = (k(x + i, y + j, 2) + (f(x, y, 2))^2$$

$$eD_b = (k(x + i, y + j, 3) + (f(x, y, 3))^2$$

If the difference between the named pixel and the unidentified pixel is lower than the threshold, all pixels belong to the same region.

c. Feature extraction

The features can then be picked using the GLCM following the segmentation process. The GLCM technology is a process for extracting statistical texture information from the second order. The method is used in a lot of applications; however, in third and high order textures, the interaction of three or more pixels is present. The GLCM is an arithmetic objective, which can eliminate the artefacts efficiently. It is very easy to discern the image quality. For the research process, the image can be separated. To eliminate the unwanted features, use the GLCM hereby. GLCM may define the frequency of the pixels in a certain precise differential region. The target and the adjacent pixel was identified by the \emptyset route l and the nearest m value unit. Usually, the value of m is single, and \emptyset might be directed. The gained directional value can then remove undesired picture characteristics. This may be defined via the GLCM process:

$$R(m,s)=G(m,s,o, \emptyset) / \sum_{m=1}^H \sum_{n=1}^H G(m,s,o, \emptyset) \quad (6)$$

Where G is the frequency vector, the frequency m, n, o is typically the pixel value of the particular component l and m, R is the picture feature of m, and l is the pixel value, \emptyset is the normalized pixel. The various properties may be accessed by implementing the GLCM.

Entropy:

This includes general information on the compact image objects.

$$\text{Entropy} = - \sum_{m=1}^{H-1} \sum_{n=1}^{H-1} R(s,o) * \log(R(s,o)) \quad (7)$$

Where R(s,o) were characteristic frequency R, H is the constant to be fixed.

Angular moment:

In summing up the data produced, the GLCM may be utilized to calibrate high to low image homogeneity. If the precision is low, the angular moment is considerable. The images are usually homogeneous.

$$\text{Angular moment} = \sum_{m=1}^{H-1} \sum_{s=1}^{H-1} R(s,o)^2 \quad (8)$$

Contrast:

The pictures are calculated by their intensity. The disparity between the areas is often evaluated.

$$\text{Contrast} = \sum_{s=0}^{H-1} s^2 \{ \sum_{s=1}^{H-1} R(s,o) \} \quad (9)$$

Inverse difference moment:

It is also used for the general measurement of homogeneity.

$$\text{IDM} = \sum_{m=1}^{H-1} \sum_{s=1}^{H-1} \frac{1}{1} + (s - o)^2 R(s,o) \quad (10)$$

Energy:

It might be used to assess the feasibility of providing as many nonlinear components as possible.

$$\text{E} = \sum_{s=0}^{H-1} \sum_{s=1}^{H-1} R(s,o)^3 \quad (11)$$

Variance:

A variation from the mean is calculable directly gray level values

$$\text{VAR} = \sum_{m=1}^{H-1} \sum_{s=1}^{H-1} (R(s,o))^3 - \emptyset^2 \quad (12)$$

Sum average:

The connections between pixels frequency may usually be found.

$$\sum_{s=0}^{2H-1} s R_{x+y(l)} \quad (13)$$

Then the characteristics may be viewed after extracting them by using the scale down bee herd optimization algorithm. It is an evolutionary technique that is mainly used for the process of evolutionary programming, evolutionary methods, and genetic programming. SDBHCO is inspired sociologically since the algorithm is based totally on sociological behaviour related to the approach of hen flocking. It is a population-dependent evolutionary algorithm that's much like the different population primarily based evolutionary algorithms, SDBHCO is used to attain the answer to a few of the random people. It is an appearance inside the form of the disorganized community of the shifting debris that generally tends to cluster collectively on an identical time as each bee can seems to be moving in an arbitrary course.

$$V_{id} = W V_{id} + C \text{rand} (P - X) + C \text{rand} (g - x) \quad (14)$$

The position of each vector is enriched with a new vector in the form of,

$$X_{id}^{t+1} = X_{id}^t + V_{id}^{t+1} \quad (15)$$

SDBHCO decreases linearly concerning optimization,



$$W_{iter_{max}} = W_{max} - \left(\frac{W_{max} - W_{min}}{iter_{max}} \right) * (16)$$

The steps in the SDBHCO algorithm

- Launch the bee herd in a particular space of the quest.
- Evaluate each herd's output.
- Equate the fitness value of the sample to the better one. Set this value as best if the amount of particles is greater than the best

The suggested optimization algorithm is split by the c fitness assignment function and then the cluster assignment throughput to minimize the features that are to pick the best features in an ideal way. The issue of optimization was devised to evaluate the best fitness features. A bee is a considerable number of alike, essential administrators partner locally among themselves and their condition, with no key control to empower an overall interesting behaviour to create. Bee herd counts have to start late come up as a gathering of nature-spurred, masses based figuring that is fit for making insignificant exertion, snappy, and solid responses for a couple of complex issues.

Algorithm 1 Scale down bee herd optimization algorithm

```

Input: Find the best possible features
Output: Specialized features
Phase 1: Find the list of features
Phase 2: Find out a job is inappropriate
End for
Phase 3: Find out the importance
End for
Phase 4: Sort out features according to their importance
Phase 5 Organize the task according to the features needed
Step 6 Sorted features
    Task sorted (Ti) Sorted Process
    If (MAX)
        Assign feature value
        Boost the features
    Else
        provide additional features
    End if
    End for
Phase 7: End
    
```

Fitness Function estimation

The following assumption is made for problems

of the best fitness solution. The first is that N and N services were given and all tasks should be one-to-one shared. The following theory is that for the whole i and j, the individual likelihood (Kij) of the ith operation being carried out until the services j-th is assigned to the ith operation is known. Therefore, consider resource distribution issues to maximize fitness function depicted by,

$$F(X) = \sum_{i=1}^N \cos T(i) \left[\prod_{j=1}^N [1 - K_{ij}]^{X_{ij}} \right] \quad (17)$$

With respect to the assumption that the entire activities should be allocated one-to-one; that is,

$$\sum_{j=1}^N X_{ij} = 1, i = 1, 2, \dots, N \quad \text{and} \quad (18)$$

$$\sum_{i=1}^N X_{ij} = 1, j = 1, 2, \dots, N \quad (19)$$

for the prediction of the j -th fitness, Xij is a Boolean value to the i-th activity, where Xij = 1 denotes that the j -th solution is allocated to the i-th activity by its best fitness features can get evaluated.

d.Classification

The training data set is used to train the learning classifiers by the classifier to learn the features of the dataset and their relationships to their predefined categories. The test dataset is entered into the classifier as the input, and the expected categories will be output for each test until the classifier is completely qualified. The classification process after choosing the features is used in the last stage for the selection of the biomedical data collection. Here the deep residual Boltzmann CNN was preferred. A deep residual Boltzmann CNN can be used to make the classification operation. DRBCNN has several attributes, and function layers are applied to determine meaningful classification outcomes. The DRBCNN function is built on the kernel, the batten functionality is classified, and the target web page was predicted. In each and every layer of kernel function is enabled here. Any linear model can be twisted by the use of a kernel trick into a nonlinear template. Both attributes are determined by kernel thresholds so that higher attributes and thresholds are provided faster. DRBCNN is chosen to classify because it has good generalization capabilities, is extremely stable and works well for actual data sets. In the preparation and research stage, the classification



process is divided. The extracted features are easily understood by example data sets in training for the developed DRBCNN. The DRBCNN classifies the data sets in unique parts as it is checked.

$$s_j^1 = \sigma \sum_k x_{jk}^1 a_k^1 + b_j^1 \quad (20)$$

The equation may be expressed as vectorized,

$$b_j^1 = \sigma(x^l a^{l-1} + b^l) \quad (21)$$

The quadratic set combines the training set,

$$q = \frac{1}{2} \|Y - a^l\|^2 = \frac{1}{2} \sum_j (y_j - a_j^l)^2 \quad (22)$$

The gradient output is given by,

$$\frac{\partial C}{\partial w_{kj}^1} =$$

$$a_k^{l-1} \delta_j^l = c \quad (23)$$

$$F = \det[sn] - k (\text{classify}(sn))^2 \quad (24)$$

Thus the transformation becomes,

Transformation =

$$\sum_{\text{text}(x,y)} [W_{\text{match}(1)} x - \frac{\text{text}}{2} / \text{match} + W_{\text{text}(2)} x - \text{data} / \text{match}] / \text{text} \text{number}(n) * \frac{1}{\sqrt{2 * \pi * \delta_{ev}^2 * \exp(\psi_{el-1})^2 \delta_{ev}^2}} \quad (25)$$

If a query has been submitted, then the multiple sub-data for each query in the database was generated. The databases are numbered with 1,2, ... and so on to the right. Then design query data of the same name in the request and the archive. MD distance for each pair to be minimized:

$$S = \frac{1}{n} \sum_{p \in P} (p - m)(p - m)^T \quad (26)$$

Finally, a ranking is generated for the matching distance of database texts,

Algorithm 2 DRBCNN

Input: Extracted features

Output: Classified valued

Step1: initialize the parameters,

(∂C)/(∂w_{kj}^l)=[Inner iteration outer iteration]

Let to abnormality computation,

```

for ii=1: τ_Li // Inner iteration
    for i=1: ψ_el //edge value
        yi=φ_cl-ψ_el
        trans= yi* yi/ [δ_ev]^2
    trans= text
    for jj=1: φ_cl*ω_gl //all labels
        t1=1/(J(2*π)* [δ_ev]^2*exp [ψ_el-1])^2 [δ_ev]^2 )
        t2=t1*0;
        for ind=1: τ_Li*τ_oi // all pixels
            k=mode (indices-1, τ_Li)+2;
            l=base ((indices-1)/ τ_Li)+2;
            m=0;
            if k-2>=2 && R(k-2,l)==0
                v=v+(1 ~ = p(k-2,i))/3;
            end
            if k+2<=m && R(k+1,l)==0
                v=v+(1 ~ = P(k+1,l))/3;
            end
            if l-2>=1 && R(k,l-2)==0
                v=v+(1 ~ = P(k,l-2))/3;
            end
            if l+1<=m && Z(k,l+1)==0
                v=v+(1 ~ = P(k,l+1))/3;
            end
            ED3(indices)=v;
        end
        M_(l,:)=ED 1.*exp(-trans2);
    γ_s=(o_classification)
    
```

RESULT AND DISCUSSION

The CT Colon pictures are used to verify the performance analysis of the suggested approach and to evaluate various targets. In the middle of the imaging of our approaches, the contrasts are high precision of the abnormal goal detection outcome.



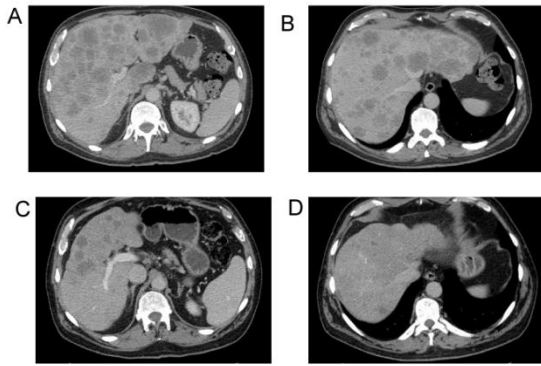


Figure 2 Sample input

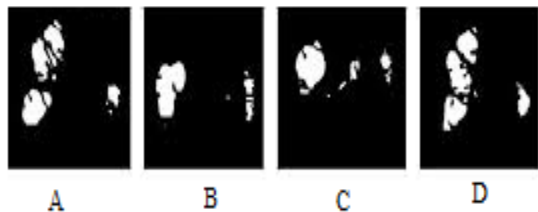


Figure 3 Segmented output

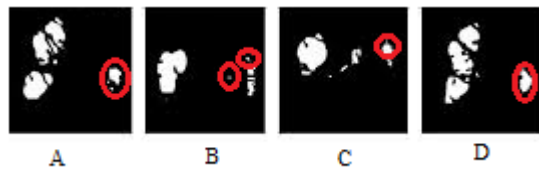


Figure 4 Classification output

Figure 2 represents the sample images from our dataset. Figure 3, in which by implementing the suggested methodology, the lymph nodes can get segmented. As of figure 4, the malicious lymph node can get classified, which helps for its removal. To prove the effectiveness of the suggested methodology, it can be compared with some other existing methods [16],[17]. Some parameters were measured and analyzed in order to assess the output. The performance analysis is conducted by means of different performance measurement methods assessed for the proposed system in contrast to the remaining research studies. Some terms are used in this analysis: (1) true positive (TP), (2) true negative (TN), (3) False-positive (Fp) and (4) false negative (FN). TP shows the usual images that are identified correctly. FP signifies photos that have been wrongly marked. TN shows abnormal images that have been properly classified. FN implies images that are mistakenly branded anomalous.

A statistical output indicator is a sensitivity. This is also a parameter of categorization, which is also considered a TP limit. In each example, the per cent of regular images is measured appropriately. The feature is often called TN. It appropriately monitors irregular images.

$$\text{Sensitivity} = \frac{TP}{TP+FN} \tag{28}$$

The specificity of the real negative measurements also refers to the quantity of the correctly detected negative.

$$\text{Specificity} = \frac{TN}{TN+FP} \tag{29}$$

Accuracy is the proportion of the number of images accurately achieved by the number of available images. The precision and accuracy of the recall are indicated in proportion.

$$\text{Accuracy (A)} = \frac{TP+TN}{TP+TN+FP+FN} \tag{30}$$

Dice co-efficient:

Can a and b be the properties of the fundamental truth data and the data characteristics found. Then the Dice coefficient was determined,

$$D(a,b) = \frac{2a \cap b}{a+b} = \frac{2TP}{2TP+FN+FP}$$

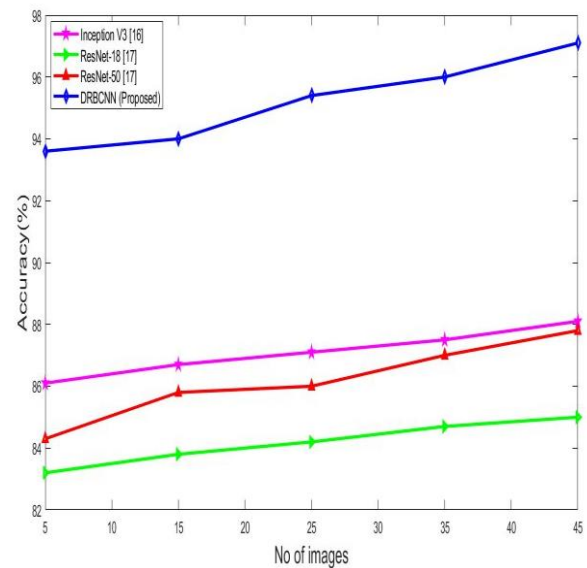


Figure 5 Number of images Vs. Accuracy

Figure 5 shows the proposed classification method, showing a maximum precision yield of 97.7%, which is better than conventional methods.



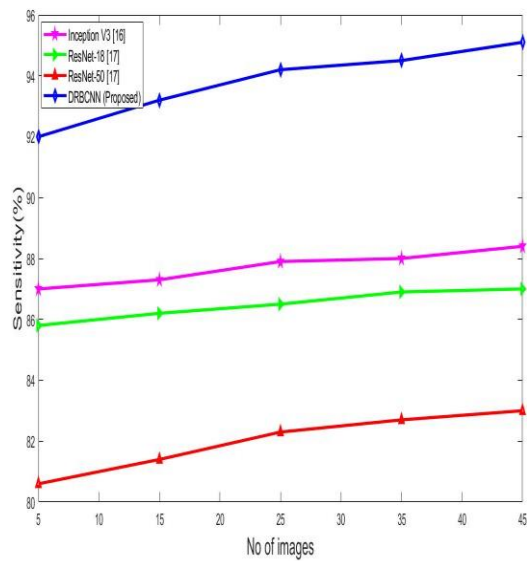


Figure 6 Number of images Vs. Sensitivity

Figure 6 graph shows the proposed system, which shows a higher sensitivity rate (95.7%) compared with the system already in use.

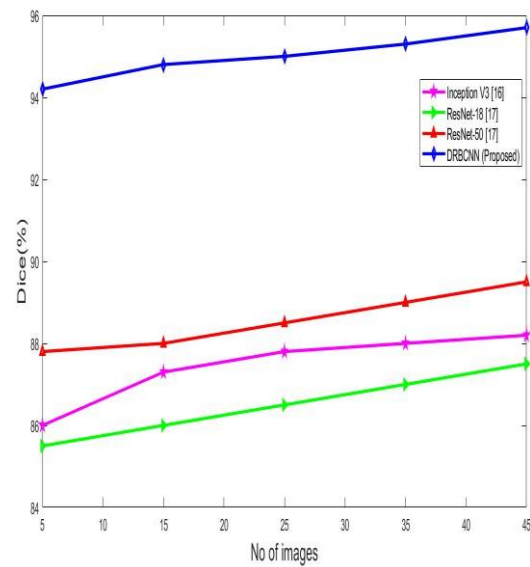


Figure 8 Number of images Vs. Dice coefficient

For the solution, figure 8 is a dice ranking. The findings reveal that the proposed method shows exact high values regarding the coefficient of dices.

6799

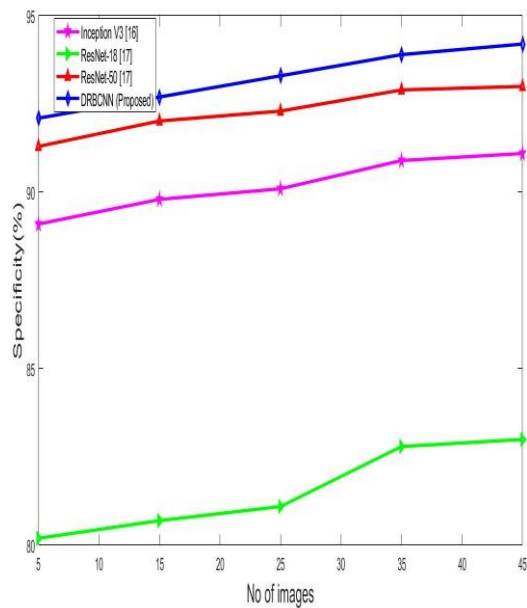


Figure 7 Number of images Vs. Specificity

The accuracy of the specificity values arrived at by the new approach is contrasted with the methods described in Figure 7. The results of the graph indicate clearly that, compared to existing methods, the method proposed produced a higher specificity rate (95.8 per cent).

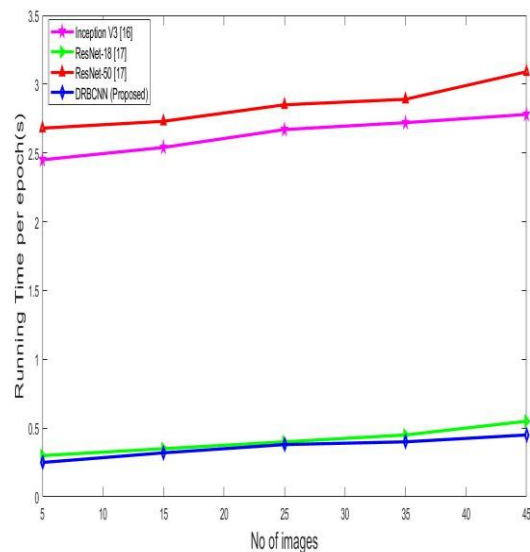


Figure 9 Number of images Vs. Running time

The computation time of the DRBCNN for classifying the data was very low (0.3 sec) when compared to the other existing classifiers, as depicted in figure 9. The findings obtained show that when compared to the existing technique, the suggested technique performs well.



CONCLUSION

All of the disease classification classifiers deliver respectable accuracy with minor marginal deviations, which isn't conclusive. A larger dataset with a greater number of categories may present the classifiers with greater difficulty and dimensionality, and there may be a clear best performer when faced with such challenges. To conduct this analysis, DRBCNN was used exclusively. On a dataset of thousands of data points, run a sequence of experiments. Based on the finding of the suggested approach, high accuracy, low false-positive rate, and high detection speed were effective in categorizing illness data. Deep learning can be utilized as a potential variation of our strategy to delete features. In the future, the suggested methodology was implemented over other types of the tumour.

References

- [1] J.-E. Ribault, P. Giraud, M. Housset, C. Durdux, J. Taieb, A. Berger, et al., "Deep Learning and Radiomics predict complete response after neoadjuvant chemoradiation for locally advanced rectal cancer," vol. 8, pp. 1-8, 2018.
- [2] H. Li, P. Bermel, J. Janopaul-Naylor, H. Zhong, Y. Xiao, E. Ben-Josef, et al., "Deep convolutional neural networks for imaging data based survival analysis of rectal cancer," in 2019 IEEE 16th International Symposium on Biomedical Imaging (ISBI 2019), 2019, pp. 846-849.
- [3] X.-Y. Zhang, L. Wang, H.-T. Zhu, Z.-W. Li, M. Ye, X.-T. Li, et al., "Predicting rectal cancer response to neoadjuvant chemoradiotherapy using deep learning of diffusion kurtosis MRI," vol. 296, pp. 56-64, 2020.
- [4] L. Ding, G. Liu, X. Zhang, S. Liu, S. Li, Z. Zhang, et al., "A deep learning nomogram kit for predicting metastatic lymph nodes in rectal cancer," vol. 9, pp. 8809-8820, 2020.
- [5] X. Fan, X. Wan, Y. Huang, H. Cai, X. Fu, Z. Yang, et al., "Epithelial-mesenchymal transition biomarkers and support vector machine guided model in preoperatively predicting regional lymph node metastasis for rectal cancer," vol. 106, pp. 1735-1741, 2012.
- [6] L.-D. Chen, J.-Y. Liang, H. Wu, Z. Wang, S.-R. Li, W. Li, et al., "Multiparametric radionics improve prediction of lymph node metastasis of rectal cancer compared with conventional radiomics," vol. 208, pp. 55-63, 2018.
- [7] X. Zheng, Z. Yao, Y. Huang, Y. Yu, Y. Wang, Y. Liu, et al., "Deep learning radiomics can predict axillary lymph node status in early-stage breast cancer," vol. 11, pp. 1-9, 2020.
- [8] D. Tse, N. Joshi, E. Anderson, M. Brady, and F. J. T. B. j. o. r. Gleeson, "A computer-aided algorithm to quantitatively predict lymph node status on MRI in rectal cancer," vol. 85, pp. 1272-1278, 2012.
- [9] P. Gupta, S.-F. Chiang, P. K. Sahoo, S. K. Mohapatra, J.-F. You, D. D. Anthony, et al., "Prediction of colon cancer stages and survival period with a machine learning approach," *Cancers*, vol. 11, p. 2007, 2019.
- [10] N. Salmi and Z. Rustam, "Naïve Bayes classifier models for predicting the colon cancer," in IOP Conference Series: Materials Science and Engineering, 2019, p. 052068.
- [11] A. A. Borkowski, C. P. Wilson, S. A. Borkowski, L. B. Thomas, L. A. Deland, and S. M. Mastorides, "Apple machine learning algorithms successfully detect colon cancer but fail to predict KRAS mutation status," arXiv preprint arXiv:1812.04660, 2018.
- [12] M. S. Kwak, H. H. Lee, J. M. Yang, J. M. Cha, J. W. Jeon, J. Y. Yoon, et al., "Deep Convolutional Neural Network-Based Lymph Node Metastasis Prediction for Colon Cancer Using Histopathological Images," *Frontiers in Oncology*, vol. 10, p. 3053, 2021.
- [13] Y. Li, A. Eresen, J. Shangguan, J. Yang, Y. Lu, D. Chen, et al., "Establishment of a new noninvasive imaging prediction model for liver metastasis in colon cancer," *American journal of cancer research*, vol. 9, p. 2482, 2019.
- [14] M. A. Horaira, M. S. Ahmed, M. H. Kabir, M. N. H. Mollah, and M. A. R. Shah, "Colon cancer prediction from gene expression profiles using kernel-based support vector machine," in 2018 International Conference on Computer, Communication, Chemical, Material and Electronic Engineering (IC4ME2), 2018, pp. 1-4.
- [15] T. Babu, T. Singh, D. Gupta, and S. Hameed, "Colon cancer prediction on histological images using deep learning features and Bayesian optimized SVM," *Journal of Intelligent & Fuzzy Systems*, pp. 1-12, 2021.
- [16] L. Xu, B. Walker, P.-I. Liang, Y. Tong, C. Xu, Y. C. Su, et al., "Colorectal cancer detection based on deep learning," *Journal of Pathology Informatics*, vol. 11, 2020.
- [17] D. Sarwinda, R. H. Paradise, A. Bustamam, and P. Anggia, "Deep Learning in Image Classification using Residual Network (ResNet) Variants for Detection of Colorectal Cancer," *Procedia Computer Science*, vol. 179, pp. 423-431, 2021.

